

Revisiting the Phase Transition of Spin-1/2 Heisenberg Model with a Spatially Staggered Anisotropy on the Square Lattice

F.-J. Jiang^{1,*}

¹*Department of Physics, National Taiwan Normal University, 88, Sec.4, Ting-Chou Rd., Taipei 116, Taiwan*

Puzzled by the indication of a new critical theory for the spin-1/2 Heisenberg model with a spatially staggered anisotropy on the square lattice as suggested in [1], we re-investigate the phase transition of this model induced by dimerization using first principle Monte Carlo simulations. We focus on studying the finite-size scaling of $\rho_{s1}L$ and $\rho_{s2}L$, where L stands for the spatial box size used in the simulations and ρ_{si} with $i \in \{1, 2\}$ is the spin-stiffness in i -direction. From our Monte Carlo data, we find that $\rho_{s2}L$ suffers a much less severe correction compared to that of $\rho_{s1}L$. Therefore $\rho_{s2}L$ is a better quantity than $\rho_{s1}L$ for finite-size scaling analysis concerning the limitation of the availability of large volumes data in our study. Further, motivated by the so-called cubical regime in magnon chiral perturbation theory, we additionally perform a finite-size scaling analysis on our Monte Carlo data with the assumption that the ratio of spatial winding numbers squared is fixed through all simulations. As a result, the physical shape of the system remains fixed in our calculations. The validity of this new idea is confirmed by studying the phase transition driven by spatial anisotropy for the ladder anisotropic Heisenberg model. With this new strategy, even from $\rho_{s1}L$ which receives the most serious correction among the observables considered in this study, we arrive at a value for the critical exponent ν which is consistent with the expected $O(3)$ value by using only up to $L = 64$ data points.

PACS numbers:

I. INTRODUCTION

Heisenberg-type models have been studied in great detail during the last twenty years because of their phenomenological importance. For example, it is believed that the spin-1/2 Heisenberg model on the square lattice is the correct model for understanding the undoped precursors of high T_c cuprates (undoped antiferromagnets). Further, due to the availability of efficient Monte Carlo algorithms as well as the increasing power of computing resources, properties of undoped antiferromagnets on geometrically non-frustrated lattices have been determined to unprecedented accuracy [2–8]. For instance, using a loop algorithm, the low-energy parameters of the spin-1/2 Heisenberg model on the square lattice are calculated very precisely and are in quantitative agreement with the experimental results [9]. Despite being well studied, several recent numerical investigation of anisotropic Heisenberg models have led to unexpected results [1, 10, 11]. In particular, Monte Carlo evidence indicates that the anisotropic Heisenberg model with staggered arrangement of the antiferromagnetic couplings may belong to a new universality class, in contradiction to the theoretical $O(3)$ universality prediction [1]. For example, while the most accurate Monte Carlo value for the critical exponent ν in the $O(3)$ universality class is given by $\nu = 0.7112(5)$ [12], the corresponding ν determined in [1] is shown to be $\nu = 0.689(5)$. Although subtlety of calculating the critical exponent ν from performing finite-size scaling analysis is demonstrated for a similar anisotropic Heisenberg

model on the honeycomb lattice [13], the discrepancy between $\nu = 0.689(5)$ and $\nu = 0.7112(5)$ observed in [1, 12] remains to be understood.

In order to clarify this issue further, we have simulated the spin-1/2 Heisenberg model with a spatially staggered anisotropy on the square lattice. Further, we choose to analyze the finite-size scaling of the observables $\rho_{s1}L$ and $\rho_{s2}L$, where L refers to the box size used in the simulations and ρ_{si} with $i \in \{1, 2\}$ is the spin stiffness in i -direction. The reason for choosing $\rho_{s1}L$ and $\rho_{s2}L$ is twofold. First of all, these two observables can be calculated to a very high accuracy using loop algorithms. Secondly, one can measure ρ_{s1} and ρ_{s2} separately. In practice, one would naturally use ρ_s which is the average of ρ_{s1} and ρ_{s2} for the data analysis. However for the model considered here, we find it is useful to analyze both the data of ρ_{s1} and ρ_{s2} because studying ρ_{s1} and ρ_{s2} individually might reveal the impact of anisotropy on the system. Surprisingly, as we will show later, the observable $\rho_{s2}L$ receives a much less severe correction than $\rho_{s1}L$ does. Hence $\rho_{s2}L$ is a better observable than $\rho_{s1}L$ (or ρ_sL) for finite-size scaling analysis concerning the limitation of the availability of large volumes data in this study. Further, motivated by the so-called cubical regime in magnon chiral perturbation theory, we have performed an additional finite-size scaling analysis on $\rho_{s1}L$ with the assumption that the ratio of spatial winding numbers squared is fixed in all our Monte-Carlo simulations. In other word, we keep the physical shape of the system fixed in the additional analysis of finite-size scaling. The validity of this new idea is confirmed by studying the phase transition driven by spatial anisotropy for the ladder anisotropic Heisenberg model, namely the critical point and critical exponent ν for this

*fjjiang@ntnu.edu.tw

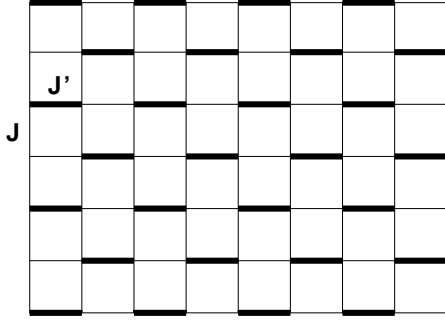


FIG. 1: The anisotropic Heisenberg model considered in this study.

phase transition we obtain by fixing the ratio of spatial winding numbers squared are consistent with the known results in the literature. Remarkably, combining the idea of fixing the ratio of spatial winding numbers squared in the simulations and finite-size scaling analysis, unlike the unconventional value for ν observed in [1], even from $\rho_{s1}L$ which suffers a very serious correction, we arrive at a value for ν which is consistent with that of $O(3)$ by using only up to $L = 64$ data points.

This paper is organized as follows. In section II, the anisotropic Heisenberg model and the relevant observables studied in this work are briefly described. Section III contains our numerical results. In particular, the corresponding critical point as well as the critical exponent ν are determined by fitting the numerical data to their predicted critical behavior near the transition. Finally, we conclude our study in section IV.

II. MICROSCOPIC MODEL AND CORRESPONDING OBSERVABLES

The Heisenberg model considered in this study is defined by the Hamilton operator

$$H = \sum_{\langle xy \rangle} J \vec{S}_x \cdot \vec{S}_y + \sum_{\langle x'y' \rangle} J' \vec{S}_{x'} \cdot \vec{S}_{y'}, \quad (1)$$

where J and J' are antiferromagnetic exchange couplings connecting nearest neighbor spins $\langle xy \rangle$ and $\langle x'y' \rangle$, respectively. Figure 1 illustrates the Heisenberg model described by Eq. (1). To study the critical behavior of this anisotropic Heisenberg model near the transition driven by spatial anisotropy, in particular to determine the critical point as well as the critical exponent ν , the spin stiffnesses in 1- and 2-directions which are defined by

$$\rho_{si} = \frac{1}{\beta L^2} \langle W_i^2 \rangle, \quad (2)$$

are measured in our simulations. Here β is the inverse temperature and L refers to the spatial box size. Further $\langle W_i^2 \rangle$ with $i \in \{1, 2\}$ is the winding number squared in i -direction. By carefully investigating the spatial volumes and the J'/J dependence of $\rho_{si}L$, one can determine the

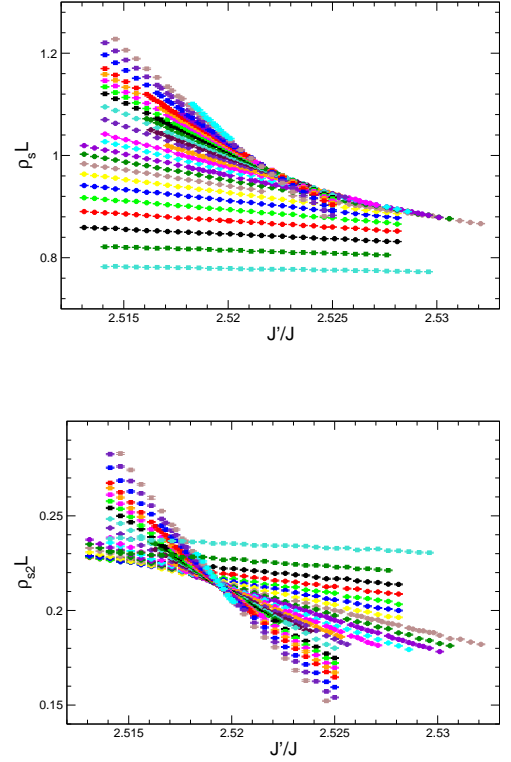


FIG. 2: Monte Carlo data of $\rho_s L$ (upper panel) and $\rho_{s2} L$ (lower panel) as functions of the parameter J'/J .

critical point as well as the critical exponent ν with high precision.

III. DETERMINATION OF THE CRITICAL POINT AND THE CRITICAL EXPONENT ν

To calculate the relevant critical exponent ν and to determine the location of the critical point in the parameter space J'/J , one useful technique is to study the finite-size scaling of certain observables. For example, if the transition is second order, then near the transition, the observable $\rho_{si}L^\nu$ for $i \in \{1, 2\}$ should be described well by the following finite-size scaling ansatz

$$\mathcal{O}_{L^p}(t) = (1 - b(L^p)^{-\omega})g_{\mathcal{O}}(t(L^p)^{1/\nu}), \quad (3)$$

where \mathcal{O}_{L^p} stands for $\rho_{si}L^\nu$, L^p is the physical linear length of the system, $t = (j_c - j)/j_c$ with $j = (J'/J)$, b is some constant, ν is the critical exponent corresponding to the correlation length ξ and ω is the confluent correction exponent. Finally $g_{\mathcal{O}}$ appearing above is a smooth function of the variable $t(L^p)^{1/\nu}$. In practice, the L^p appearing in Eq. (3) is conventionally replaced by the box size L used in the simulations when performing finite-size scaling analysis. We will adopt this conventional strategy in the first part of our analysis as well. From Eq. (3), one concludes that the curves of different L for \mathcal{O}_L , as functions of J'/J , should have the tendency to intersect at critical point $(J'/J)_c$ for large L . To calculate the critical

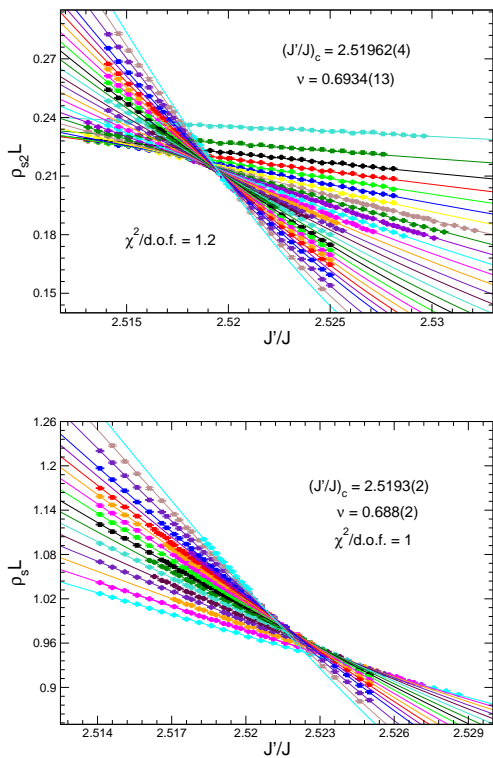


FIG. 3: Fits of $\rho_{s2}L$ (upper panel) and ρ_sL (lower panel) to Eq. (3). While the circles and squares on these two panels are the numerical Monte Carlo data from the simulations, the solid curves are obtained by using the results from the fits.

exponent ν and the critical point $(J'/J)_c$, in the following we will apply the finite-size scaling formula, Eq. (3), to both $\rho_{s1}L$ and $\rho_{s2}L$. Without losing the generality, in our simulations we have fixed J to be 1.0 and have varied J' . Further, the box size used in the simulations ranges from $L = 6$ to $L = 64$. We also use large enough β so that the observables studied here take their zero-temperature values. Figure 2 shows the Monte Carlo data of ρ_sL and $\rho_{s2}L$ as functions of the parameter J'/J . The figure clearly indicates the phase transition is likely second order since different L curves for both ρ_sL and $\rho_{s2}L$ tend to intersect at a particular point in the parameter space J'/J . What is the most striking observation from our results is that the observable ρ_sL receives a much severe correction than $\rho_{s2}L$ does. This can be understood from the trend of the crossing among these curves of different L in figure 2. Therefore one expects a better determination of ν can be obtained by applying finite-size scaling analysis to $\rho_{s2}L$. Before presenting our results, we would like to point out that since data from large volumes might be essential in order to determine the critical exponent ν accurately as suggested in [13], we will use the strategy employed in [13] for our data analysis as well. A Taylor expansion of Eq. (3) up to fourth order in $tL^{1/\nu}$ is used to fit the data of $\rho_{s2}L$. The critical exponent ν and critical

point $(J'/J)_c$ calculated from the fit using all the available data of $\rho_{s2}L$ are given by 0.6934(13) and 2.51962(4), respectively. The upper panel of figure 3 demonstrates the result of the fit. Notice both ν and $(J'/J)_c$ we obtain are consistent with the corresponding results found in [1]. By eliminating some data points of small L , we can reach a value of 0.700(3) for ν by fitting $\rho_{s2}L$ with $L \geq 26$ to Eq. (3). On the other hand, with the same range of L ($L \geq 26$), a fit of ρ_sL to Eq. (3) leads to $\nu = 0.688(2)$ and $(J'/J)_c = 2.5193(2)$, both of which are consistent with those obtained in [1] as well (lower panel in figure 3). By eliminating more data points of ρ_sL with small L , the values for ν and $(J'/J)_c$ calculated from the fits are always consistent with those quoted above. What we have shown clearly indicates that one would suffer the least correction by considering the finite-size scaling of the observable $\rho_{s2}L$. As a result, it is likely one can reach a value for ν consistent with the $O(3)$ prediction, namely $\nu = 0.7112(5)$ if large volume data points for ρ_{s2} are available. Here we do not attempt to carry out such task of obtaining data for $L > 64$. Instead, we employ the technique of fixing the ratio of spatial winding numbers squared in the simulations. Surprisingly, combining this new idea and finite-size scaling analysis, even from the observable $\rho_{s1}L$ which is found to receive the most severe correction among the observables considered here, we reach a value for the critical exponent ν consistent with $\nu = 0.7112(5)$ without additionally obtaining data points for $L > 64$. The motivation behind the idea of fixing the ratio of spatial winding numbers squared in the simulations is as follows. First of all, as we already mentioned earlier that the box size L used in the simulations is conventionally used as the L^p in Eq. (3) when carrying out finite-size scaling analysis. For isotropic systems, such strategy is no problem. However, for anisotropic cases, the validity of this common wisdom of treating L as L^p is not clear. In particular, the same L does not stand for the same L^p of the system for two different anisotropies J'/J . Hence one needs to find a physical quantity which can really characterize the physical linear length of the system. Secondly, in magnon chiral perturbation theory which is the low-energy effective field theory for spin-1/2 antiferromagnets with $O(N)$ symmetry, an exactly cubical space-time box is met when the condition $\beta c = L$ is satisfied, here c is the spin-wave velocity and β , L are the inverse temperature and box size as before. For spin-1/2 XY model on the square lattice, for large box size L , the numerical value of c determined by L/β using the β with which one obtains $\langle W^2 \rangle = 1/2(\langle W_1^2 \rangle + \langle W_2^2 \rangle) = \langle W_t^2 \rangle$ in the Monte Carlo simulations agrees quantitatively with the known results in the literature [14]. This result implies that the squares of winding numbers are more physical than the box sizes since an exactly cubical space-time box is reached when the squares of spatial and temporal winding numbers are tuned to be the same in the Monte Carlo simulations. Consequently the physical linear lengths of the system should be characterized by the

squares of winding numbers, not the box sizes used in the simulations. Based on what we have argued, it is $\langle W_1^2 \rangle / \langle W_2^2 \rangle$, not $(L_2/L_1)^2$, plays the role of the quantity $(L_2^p/L_1^p)^2$ for the system, here again we refer L_i^p with $i \in \{1, 2\}$ as the physical linear length of the system in i -direction. As a result, fixing the ratio of spatial winding numbers squared in the simulations corresponds to the situation that the physical shape of the system remains fixed in all calculations. Indeed it is demonstrated in [3] that rectangular lattice is more suitable than square lattice for studying the spatially anisotropic Heisenberg model with different antiferromagnetic couplings J_1 , J_2 in 1- and 2-directions. The idea of fixing the ratio of spatial winding numbers squared quantifies the method used in [3].

The method of fixing the ratio of spatial winding numbers squared is employed as follows. First of all, we perform a trial simulation to determine a fixed value for the ratio of spatial winding numbers squared which we denote by w_f and will be used later in all calculations. Secondly, instead of fixing the aspect ratio of box sizes L_1 and L_2 in the simulations as in conventional finite-size scaling studies, we vary the variables L_1 , L_2 and J'/J in order to satisfy the condition of a fixed ratio of spatial winding numbers squared. This step involves a controlled interpolation on the raw data points. In practice, for a fixed L_2 one performs simulations for a sequence $L_1 = L_2, L_2 \pm 2, L_2 \pm 4, \dots$. The criterion of a fixed ratio of spatial winding numbers squared is reached by tuning the parameter J_2/J_1 and then carrying out a linear interpolation based on $(w/w_f)^{(-1/2)}$ for the desired observables, here w refers to the ratio of spatial winding numbers squared of the data points other than the trial one. Notice since only the ratio of the physical linear lengths squared is fixed, it is natural to use L_2 in the finite-size scaling ansatz Eq. (3) both for the analysis of ρ_{s1} and ρ_{s2} . The validity of this unconventional finite-size scaling method can be verified by considering the transition induced by dimerization for the Heisenberg model with a ladder pattern anisotropic couplings (figure 4). For $b \sim 0.95(22)$ in Eq. (3), we obtain a good data collapse for the observable $(\rho_{s1})_{\text{in}} L_1^p (= (\rho_{s1})_{\text{in}} L_2)$. Above the subscript ‘‘in’’ means the data points are the interpolated one. To make sure that the step of interpolation leads to accurate results, we have carried out several trial simulations and have confirmed that the interpolated data points are reliable as long as the ratio is kept small (table 1). On the other hand, for $b = 1.30(18)$ in Eq. (3), a good data collapse is also obtained for the observable $\rho_{s1} L_1$, here ρ_{s1} are the raw data determined from the simulations directly. Figure 5 shows a comparison between the data collapse obtained by using the new unconventional method introduced above (upper panel) and by the conventional method (lower panel). For obtaining figure 5, we have fixed $\nu = 0.7112$, $\omega = 0.78$, and $(J/J')_c = 0.52367$, which are the established values for these quantities. As one sees in figure 5, the quality of the data collapse obtained with the new method is bet-

| J'/J | L_1 | L_2 | w_f/w | $(\rho_{s1})_{\text{in}}$ | ρ_{s1} |
|--------|-------|-------|------------|---------------------------|----------------|
| 0.53 | 96 | 96 | 0.9558(33) | 0.008188(22) | 0.008198(7) |
| 0.53 | 96 | 94 | 0.9549(32) | 0.008391(21) | 0.0084098(74) |
| 0.545 | 90 | 94 | 0.9594(35) | 0.016862(33) | 0.016835(15) |
| 0.545 | 90 | 90 | 0.9539(36) | 0.017651(35) | 0.017676(17) |
| 0.535 | 98 | 98 | 0.9591(28) | 0.011707(28) | 0.0117297(124) |
| 0.54 | 96 | 96 | 0.9592(29) | 0.014838(37) | 0.014846(13) |
| 0.525 | 96 | 96 | 0.9503(41) | 0.0072255(225) | 0.0072579(66) |

TABLE I: Comparison between interpolated and original values of ρ_{s1} for several data points. The data points which are used for interpolation are obtained from the simulations with $L_1 \times (L_2 + 2)$ (except the last row which is obtained from a simulation with $(L_1 + 2) \times L_2$). The inverse temperature β for these data points are fixed to $\beta J = 800$.

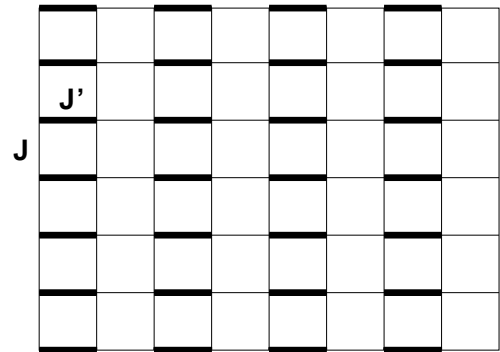


FIG. 4: Heisenberg model with a ladder pattern of anisotropy.

ter than the one obtained with the conventional method, thus confirming the validity of the idea to fix the ratio of winding numbers squared in order to studying the critical theory of a second order phase transition.

As demonstrated above, in general for a fixed L_2 , one can vary L_1 and J'/J in order to reach the criterion of a fixed aspect-ratio of spatial winding numbers squared in the simulations. For our study here, without obtaining additional data, we proceed as follows. First of all, we calculate the ratio $\langle W_1^2 \rangle / \langle W_2^2 \rangle$ for the data point at $J'/J = 2.5196$ and $L = 40$ which we denote by w_f . We further choose $L_1^p = L$ in our data analysis. After obtaining this number, a linear interpolation for ρ_{s1} of other data points based on $(w/w_f)^{(-1/2)}$ is performed in order to reach the criterion of a fixed ratio of spatial winding numbers squared in the simulations. The w appearing above is again the corresponding $\langle W_1^2 \rangle / \langle W_2^2 \rangle$ of other data points. Here a controlled interpolation similar to what we have done in studying the ladder anisotropic Heisenberg model is performed as well. Further, since large volumes data is essential for a quick convergence of ν as suggested in [13], we make sure the set of interpolated data chosen for finite-size scaling analysis contains sufficiently many points from large volumes as long as the interpolated results are reliable. A fit of the inter-

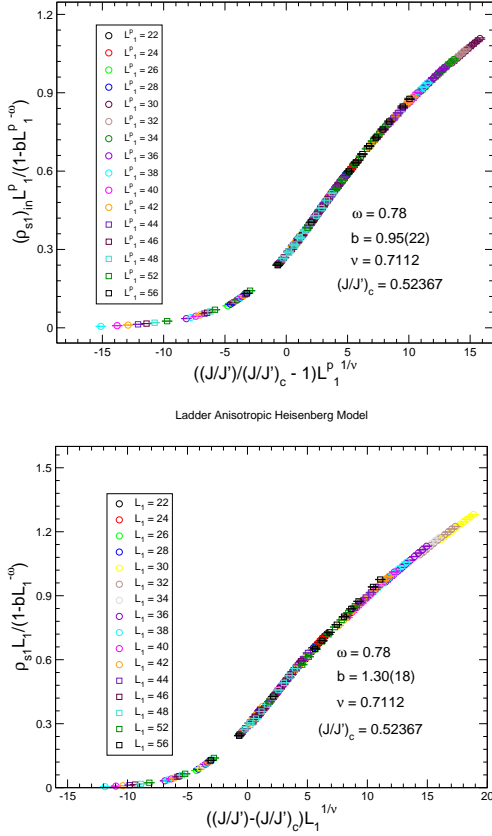


FIG. 5: Comparison between the results of data collapse using the new unconventional finite-size scaling method (upper panel) described in the text and the conventional method (lower panel) for the ladder anisotropic Heisenberg model. The result in the upper panel is obtained from simulations with box sizes $(L_2 - 6) \times L_2$, $(L_2 - 4) \times L_2$, ..., $(L_2 + 4) \times L_2$ for various values of J_2/J_1 if the interpolations from such simulations are reliable.

polated $(\rho_{s1})_{in}L$ data to Eq. (3) with ω being fixed to its $O(3)$ value ($\omega = 0.78$) leads to $\nu = 0.706(7)$ and $(J'/J)_c = 2.5196(1)$ for $36 \leq L \leq 64$ (figure 5). Letting ω be a fit parameter results in consistent $\nu = 0.707(8)$ and $(J'/J)_c = 2.5196(7)$. Further, we always arrive at consistent results with $\nu = 0.706(7)$ and $(J'/J)_c = 2.5196(1)$ from the fits using $L > 36$ data. The value of ν we calculate from the fit is in good agreement with the expected $O(3)$ value $\nu = 0.7112(5)$. The critical point $(J'/J)_c = 2.5196(1)$ is consistent with that found in [1] as well. To avoid any bias, we perform another analysis for the raw $\rho_{s1}L$ data with the same range of L and J'/J as we did for the interpolated data. By fitting this set of original data points to Eq. (3) with a fixed $\omega = 0.78$, we arrive at $\nu = 0.688(7)$ and $(J'/J)_c = 2.5197(1)$ (figure 6), both of which again agree quantitatively with those determined in [1]. Similarly, applying this unconventional finite-size scaling to ρ_{s2} would lead to a numerical value of ν consistent with $\nu = 0.7112(5)$. For instance, the ν determined by fitting $(\rho_{s2})_{in}L$ to Eq. (3) is found to be $\nu = 0.706(7)$, which agrees quantitatively

with the predicted $O(3)$ value (figure 8). Finally we would like to make a comment regarding the choice of w_f . In principle one can use w_f determined from any L and from any J'/J close to $(J'/J)_c$. However it will be desirable to choose w_f such that the set of interpolated data used for analysis includes as many data points from large volumes as possible. Using the w_f obtained at $J'/J = 2.5191$ ($J'/J = 2.5196$) with $L = 40$ ($L = 44$), we reach the results of $\nu = 0.704(7)$ and $(J'/J)_c = 2.5196(1)$ ($\nu = 0.705(7)$ and $(J'/J)_c = 2.5196(1)$) from the fit with a fixed $\omega = 0.78$. These values for ν and $(J'/J)_c$ agree with what we have obtained earlier. Indeed as we will demonstrate in another investigation, the critical exponent ν determined by the idea of fixing the ratio of spatial winding number squared in the simulations is independence of the chosen reference point.

IV. DISCUSSION AND CONCLUSION

In this paper, we revisit the phase transition driven by dimerization for the spin-1/2 Heisenberg model with a spatially staggered anisotropy on the square lattice. We find that the observable $\rho_{s2}L$ suffers a much less severe correction compared to that of $\rho_{s1}L$, hence is a better quantity for finite-size scaling analysis. Further, we propose an unconventional finite-size scaling method, namely we fix the ratio of spatial winding numbers squared. As a result, the physical shape of the system remains fixed in all simulations and analysis. With this new strategy, we arrive at $\nu = 0.706(7)$ for the critical exponent ν which is consistent with the most accurate Monte Carlo $O(3)$ result $\nu = 0.7112(5)$ by using only up to $L = 64$ data points derived from both $\rho_{s1}L$ and $\rho_{s2}L$. Interestingly, the $\chi^2/\text{d.o.f.}$ obtained from the fits using the interpolated data are better than those resulted from the fits using the raw data (figures 6, 7 and 8). This observation provides another evidence to support the quantitative correctness of the new unconventional finite-size scaling we proposed here.

It seems that when carrying out the finite-size scaling analysis for the observables considered here, the use of physical linear lengths of the system, which are characterized by the spatial winding numbers squared, would lead to a faster convergence of ν . It will be interesting to apply a similar technique to other observables such as Binder cumulants as well. However, for Binder cumulants, the correction from interpolation will cancel out because of the definition of these observables. Therefore to further test the philosophy behind the unconventional finite-size scaling method proposed here might require some new ideas. Nevertheless, with this new unconventional finite-size scaling method, we have successfully solved the puzzle raised in [1] by showing that the anisotropy driven phase transition for the spin-1/2 Heisenberg model with a staggered spatial anisotropy indeed belongs to the $O(3)$ universality class. Of course, the conventional finite-size scaling analysis is more convenient since one does not need to carry out interpolation on the raw data. How-

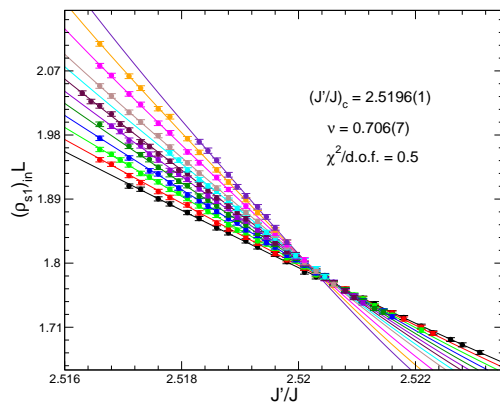


FIG. 6: Fit of interpolated $(\rho_{s1})_{in}L$ data to Eq. (3). While the circles are the numerical Monte Carlo data from the simulations, the solid curves are obtained by using the results from the fit.

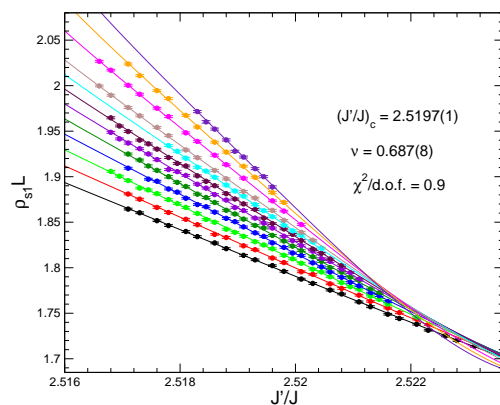


FIG. 7: Fit of original $\rho_{s1}L$ data to Eq. (3). While the circles are the numerical Monte Carlo data from the simulations, the solid curves are obtained by using the results from the fit.

ever for the subtle phase transition considered in this study, without obtaining data of gigantic lattices, a new idea which is more physical oriented such as the one presented here is necessary. Still, to clarify the puzzle of an unconventional phase transition for the model studied here as observed in [1] by simulating larger lattices and using the conventional finite-size scaling method is desirable. However, such investigation is beyond the scope of our study.

Acknowledgements

The simulations in this study are based on the loop algorithms available in ALPS library [15] and were carried out on personal desktops. Part of the results presented in this study has appeared in arXiv:0911.0653 and was done at “Center for Theoretical Physics, Massachusetts Institute of Technology, 77 Massachusetts Ave, Cambridge, MA 02139, USA “. Partial support from DOE and NCTS (North) as well as useful discussion with U. J. Wiese are acknowledged.

-
- [1] S. Wenzel, L. Bogacz, and W. Janke, Phys. Rev. Lett. **101**, 127202 (2008).
 - [2] A. W. Sandvik, Phys. Rev. B **56**, 11678 (1997).
 - [3] A. W. Sandvik, Phys. Rev. Lett. **83**, 3069 (1999).
 - [4] Y. J. Kim and R. Birgeneau, Phys. Rev. B **62**, 6378 (2000).
 - [5] L. Wang, K. S. D. Beach, and A. W. Sandvik, Phys. Rev. B **73**, 014431 (2006).
 - [6] F.-J. Jiang, F. Kämpfer, M. Nyfeler, and W.-J. Wiese, Phys. Rev. B **78**, 214406 (2008).
 - [7] A. F. Albuquerque, M. Troyer, and J. Oitmaa, Phys. Rev. B **78**, 132402 (2008).
 - [8] S. Wenzel and W. Janke, Phys. Rev. B **79**, 014410 (2009).
 - [9] U.-J. Wiese and H.-P. Ying, Z. Phys. B **93**, 147 (1994).
 - [10] T. Pardini, R. R. P. Singh, A. Katanin and O. P. Sushkov, Phys. Rev. B **78**, 024439 (2008).
 - [11] F.-J. Jiang, F. Kämpfer, and M. Nyfeler, Phys. Rev. B **80**, 033104 (2009).
 - [12] M. Campostrini, M. Hasenbusch, A. Pelissetto, P. Rossi, and E. Vicari, Phys. Rev. B **65**, 144520 (2002).
 - [13] F.-J. Jiang and U. Gerber, J. Stat. Mech. P09016 (2009).
 - [14] F.-J. Jiang, arXiv:1009.6122.
 - [15] A. F. Albuquerque et. al, Journal of Magnetism and Magnetic Material **310**, 1187 (2007).

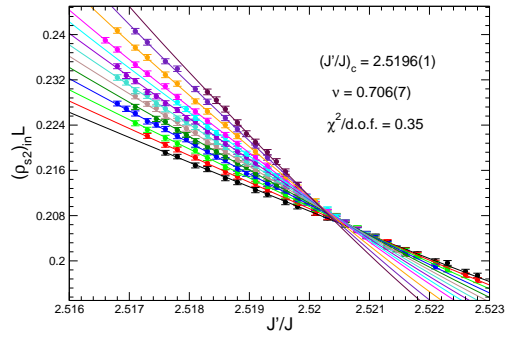


FIG. 8: Fit of interpolated $(\rho_{s2})_{in} L$ data to Eq. (3). While the circles are the numerical Monte Carlo data from the simulations, the solid curves are obtained by using the results from the fit.